

Buildup of Thermoset and Crystallization of Thermoplastics Studied by Electrical Techniques

K. FRIEDRICH,¹ C. VINH-TUNG,² G. BOITEUX,² G. SEYTRE,² J. ULAŃSKI¹

¹ Division of Polymer Physics, Institute of Polymers, Technical University of Lodz, 90-924 Lodz, Poland

² Laboratoire d'Etude des Matériaux Plastiques et des Biomatériaux, UMR CNRS No. 5627, Université Claude Bernard, Lyon I, Bât. 303, 43 Boulevard du 11 Novembre 1918, 69622 Villeurbanne Cedex, France

Received 19 July 1996; accepted 16 January 1997

ABSTRACT: Up to now, few techniques were available that allowed nondestructive *in situ* characterization of polymerization during the curing of a thermoset resin. Dynamic dielectric measurements made over a wide range of frequencies provide a sensitive and convenient control to follow up the epoxy-amine cure or to follow the formation of the thermoplastic materials. The direct current measurements and the time of flight measurements were developed to confirm interpretation of the electrical techniques in terms of correlations of the evolution of the conductivity and the network formation and also to evaluate the real value of the ion mobility and its evolution in a course of reaction. © 1997 John Wiley & Sons, Inc. *J Appl Polym Sci* **65**: 2529–2543, 1997

Key words: neat or toughened epoxy-amine; crystallization of thermoplastic; network formation; *in situ* electric monitoring, control of cure; alternative and direct current measurements; ionic carriers mobility; ion conductivity; time of flight of ionic carriers

INTRODUCTION

The ability to predict and monitor polymer processing operations is an important aspect in the development and control of polymer material fabrication. The epoxy resins provide a unique combination of properties that make them one of the most important polymer groups that have a wide range of applications where high performance in terms of resistance to chemicals and mechanical and electrical properties is required. The uncured epoxies are thermoplastic, but they

can be transformed into insoluble and infusible form by 3-dimensional (3-D) crosslinking as an effect of complex chemical reactions between the functional groups of the resin and the hardener occurring at adequate temperature. These processes are accompanied by changes of the physical properties of the system connected with phase transitions: gelation and/or vitrification. An important problem is the determination of the viscosity of the reacting system *in situ* as a function of curing time and temperature, because direct on-line measurements of viscosity are usually not possible.

In recent years electrical techniques like microdielectrometry^{1–7} attracted increasing interest because they allow continuous monitoring of advancement of the reaction of the curing resin in a nondestructive way. These methods are already used in the plastic industry. To generalize these methods for the different kinds of resins and for different processing techniques, it is important to

Correspondence to: Dr. G. Boiteux.

Contract grant sponsor: Polish State Committee for Scientific Research; contract grant number: 607/T08/96/10.

Contract grant sponsor: MRES (Ministry of Research and Educations).

Contract grant sponsor: DRET (Army)

Contract grant sponsor: Society Brochier.

Journal of Applied Polymer Science, Vol. 65, 2529–2543 (1997)

© 1997 John Wiley & Sons, Inc.

CCC 0021-8995/97/122529-15

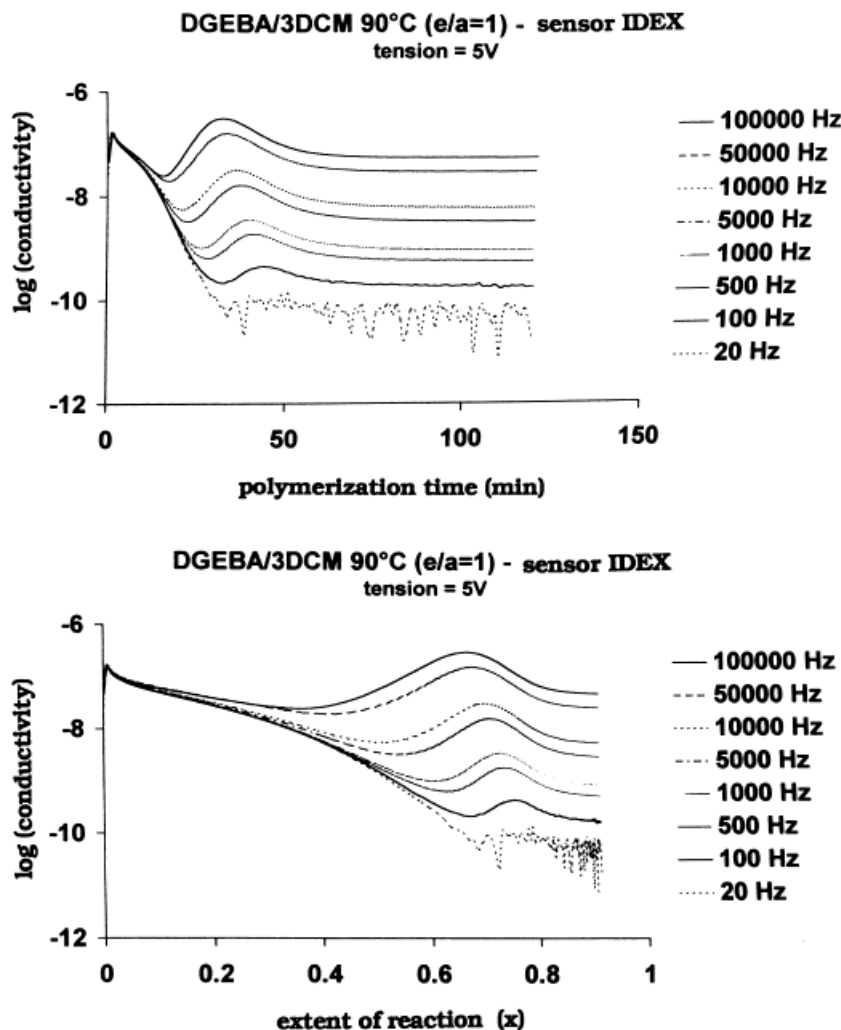


Figure 1 $\log \sigma$ at different frequencies versus time or versus conversion degree x for epoxy system DGEBA-3DCM at 90°C with IDEX sensor.

understand the physical basics of the observed phenomena during the curing process.

In a polymer system viscosity and ion conductivity are, respectively, macroscopic and microscopic properties that characterize the chain segment's mobility and the ion mobility, respectively. In general an inverse proportionality between viscosity and ion conductivity is assumed.^{2,7-9} However, the studies performed so far on the ion conductivity of the polymer systems undergoing phase transitions^{2,3,5,6,8-11} do not allow the determination of the relationships between ion conductivity, viscosity, and changes in the polymer system during all of the cure time.

Ionic conductivity is determined by the concentration of ions and their mobility. It is known that these quantities can be influenced by the chemical

structure of polymers, incorporated salt species, and, in the solid state, by morphology (e.g., degree of crystallinity).¹²⁻¹⁵ Several groups claimed that close correlations were found between evolution of the ionic conductivity and an advancement of the network formation during resin cure, allowing the determination of the occurrence of gelation and/or vitrification.¹⁶⁻¹⁸ However, it is still not well recognized how variables such as polymer structure, polymer chain length, and crosslinking density affect the ion mobility and the ion concentration, and therefore the ion conductivity. In particular, it is difficult to explain how the occurrence of gelation, which influences the macroscopic viscosity, may affect the ionic conductivity that is dependent on local, microscopic viscosity.

Developing biphasic materials to improve the

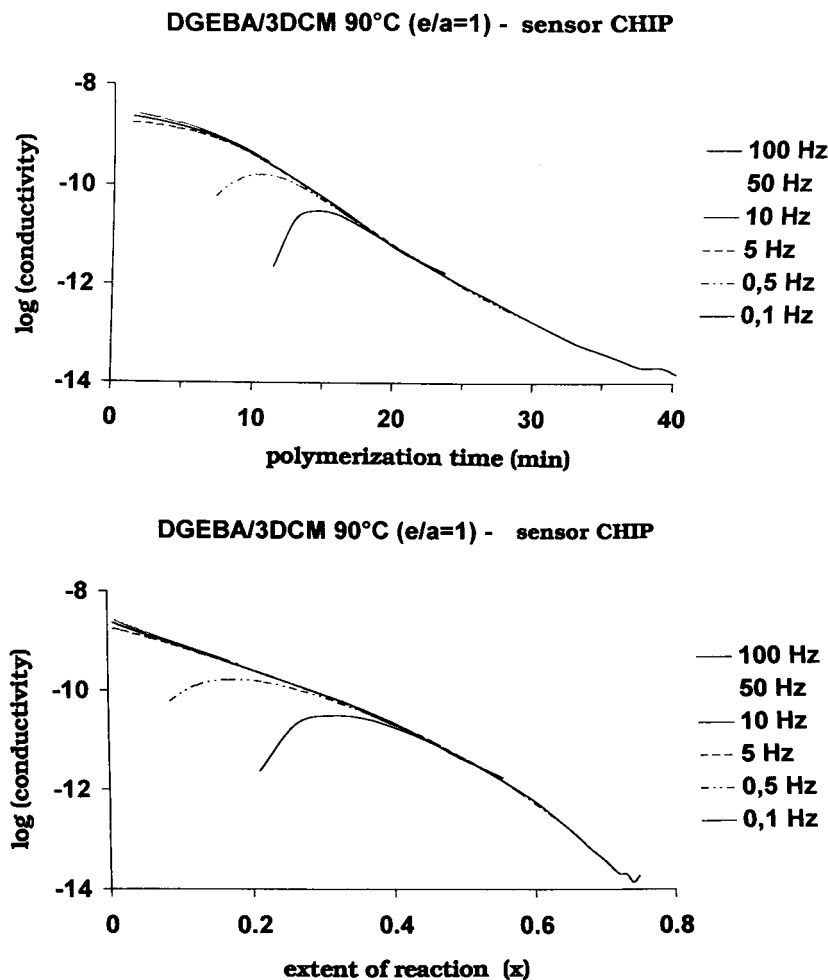


Figure 2 $\log \sigma$ at different frequencies versus time or versus conversion degree x for epoxy system DGEBA-3DCM at 90°C with CHIP sensor.

fracture toughness of thermoset resins is now a common practice. The miscibility is controlled by the temperature, molar masses, and proportions in the blend. The final morphology results from the competition between the kinetics of the reaction and the phase separation. Dielectric measurements are very useful for *in situ* monitoring of the kinetics of epoxy-amine polymerization. Recently the same measurements were made with elastomer-epoxy blends, and it was shown that the phase separation induced an interfacial polarization that was detected on the dielectric spectra.^{4,7,19} In thermoplastic-epoxy blends this interfacial polarization was observed only at the end of the polymerization, with a phase inverted morphology.^{10,20} Two of the aims of this article are to show how microdielectrometry can be used to detect phase separation in high glass

transition temperature (T_g) thermoplastic-epoxy blends^{21,22} and to monitor the cure of such systems.

The use of microdielectrometry for *in situ* monitoring of chemical reactions can be extended to physical phenomena such as crystallization. Recently, some studies were conducted for this purpose²³⁻²⁵ and concerned the changes in the long-range motions occurring above the glass transition temperature due to growing of the crystals during isothermal crystallization. On the other hand, as far as the electrical properties are concerned, the effect of the crystallinity is to lower the conductivity.^{26,27} If the conduction is ionic the ion mobility through the crystalline regions will be decreased. This type of conduction was frequently invoked to account for the low but finite conductivity of many of the more insulating poly-

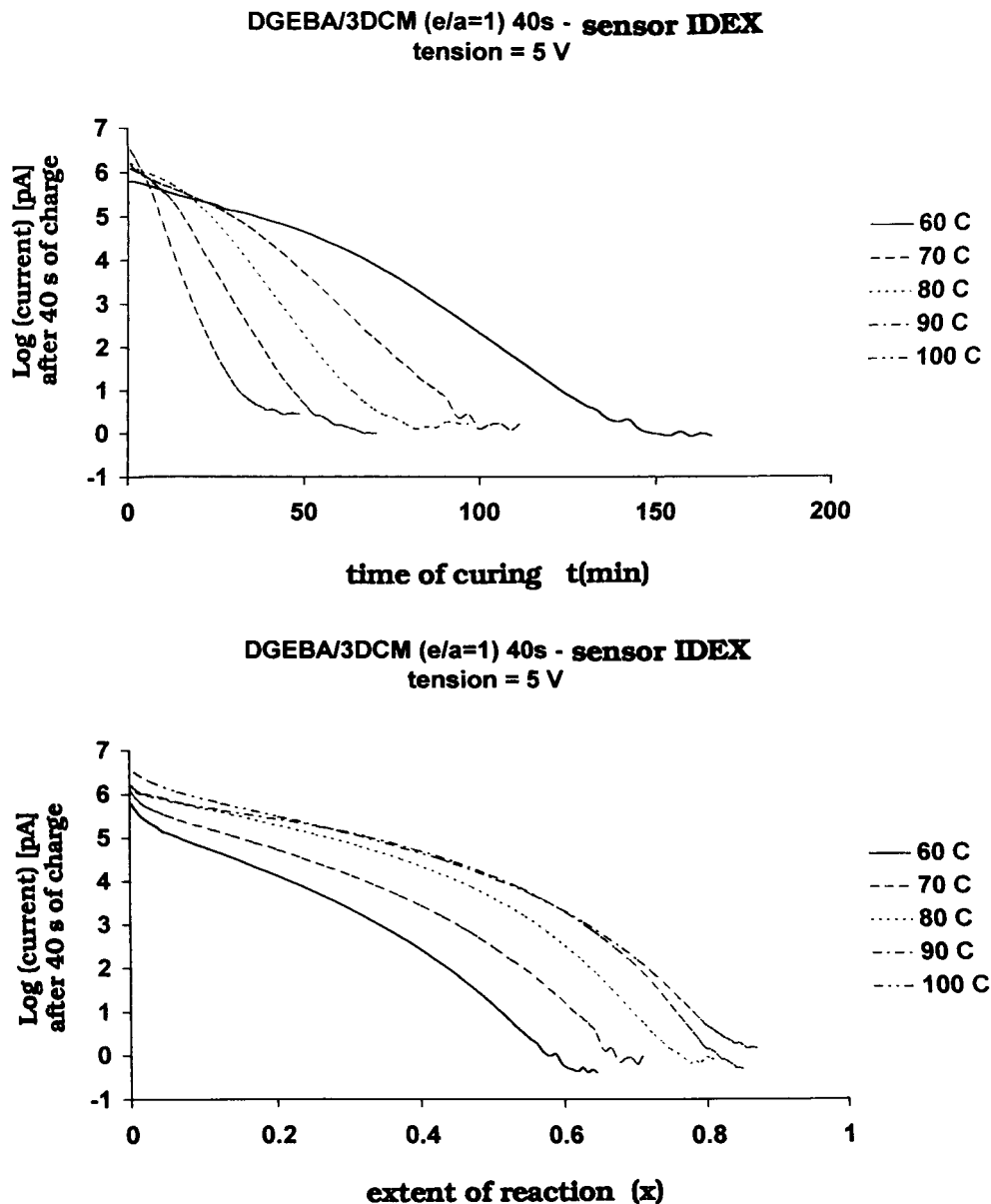


Figure 3 $\log \sigma$ for five isotherms versus time or versus conversion degree x for epoxy system DGEBA-3DCM at 90°C with IDEX sensor.

mers. If conduction is electronic it will perhaps be faster, but the crystalline amorphous interface may act as a trapping region giving a Maxwell–Wagner–Sillars (MWS) interfacial polarization.

To gain a fundamental understanding of the correlation between electrical and chemorheological phenomena, the mechanism of ionic conduction in reactive polymers has to be clarified. This means that not only the changes of the conductivity but also the evolution of fundamental physical

quantities (concentrations and origin of mobile ions and their mobility) have to be investigated.

EXPERIMENTAL

Electrical Measurements

Microdielectrometry Measurements

For dielectric analysis the electrode configuration was an interdigitated comb pattern and a small

amount of the reactive system to be studied was layered over the sensitive area. Two different probes were used: a “ceramic single surface sensor” and an “IDEX sensor.” The ceramic sensor is a gold interdigitated comb electrode patterned onto a ceramic substrate; the IDEX sensor consists of nickel electrodes deposited onto a polyimide (kapton) substrate. Dielectric scans were recorded using a DEA TA 2970 for the ceramic single surface sensor and a Micromet Instruments Eumetric System III microdielectrometer for the IDEX sensor. In the IDEX case simultaneous dielectric and cloud point isothermal measurements were possible by monitoring the light intensity transmitted through the sample. Additionally, some dielectric experiments were carried out with a Polymer Laboratories apparatus linked with 4284 HP bridge. All these dielectric systems generated sinusoidal signals in the frequency range between 10^{-2} Hz and 100 kHz.

Dielectric analysis is based on the study of the electrical response of a curing polymer placed on the sensor undergoing the alternative electric field stress. The output current is attenuated and out of phase compared with the output voltage. The response of such an imperfect dielectric material results from its capacitive component (characterized by the relative permittivity ε') and its con-

ductive component (characterized by the loss factor ε''). Three main phenomena contribute to the electrical behavior of the sample: orientation and vibration of the permanent dipoles under alternative electric field, the ionic displacements inside the dielectric material due to the impurities, and the ion charges blocking phenomena at low frequencies.

Values of ε' and ε'' are calculated by equations that quantify the relationships of one dipolar process but, in fact, it is necessary to characterize real systems in terms of a distribution of relaxation times.

$$\varepsilon' = \varepsilon'_{\text{ion}} + \varepsilon'_{\text{dipole}}$$

$$\varepsilon'' = \varepsilon''_{\text{ion}} + \varepsilon''_{\text{dipole}}$$

$$\varepsilon'_{\text{ion}} = \frac{A}{\omega^{(n+1)}} \left(\frac{\sigma}{\varepsilon_0} \right)^2$$

$$\varepsilon'_{\text{dipole}} = \varepsilon_u + \frac{\varepsilon_r - \varepsilon_u}{1 + (\omega\tau)^2}$$

$$\varepsilon''_{\text{ion}} = \frac{\sigma}{\varepsilon_0\omega} - \frac{B}{\omega^{(n+1)}} \left(\frac{\sigma}{\varepsilon_0} \right)^2$$

$$\varepsilon''_{\text{dipole}} = \frac{\omega\tau(\varepsilon_r - \varepsilon_u)}{1 + (\omega\tau)^2} \quad (1)$$

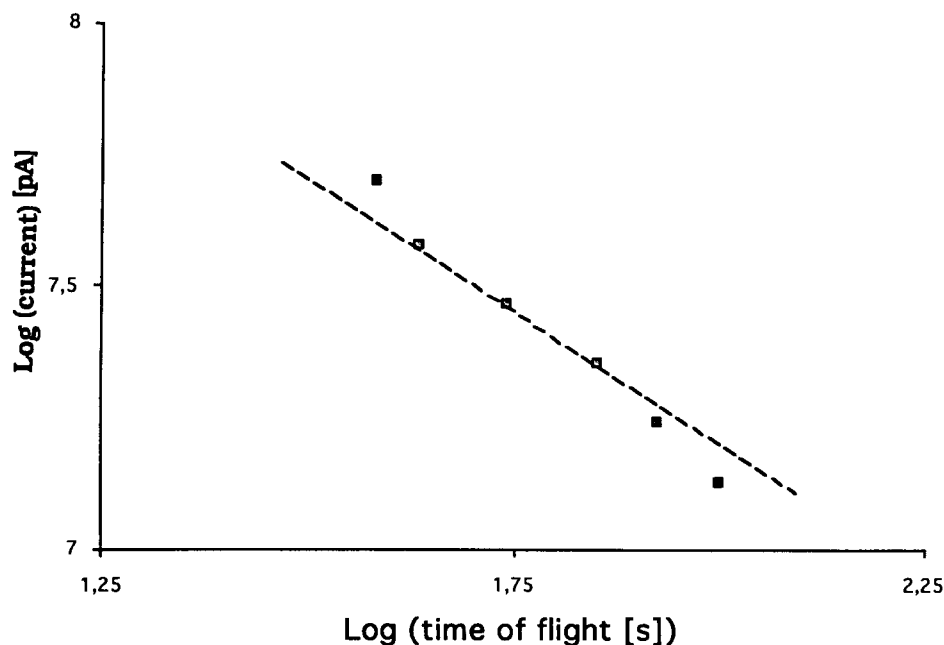


Figure 4 Plot of the ionic current values after 10 s of polarization versus time of flight τ for the DGEBA-3DCM system cured isothermally at 50°C (Cu electrodes, $d = 20$ mm, $U = 100$ V); the broken line indicates the slope -1 .

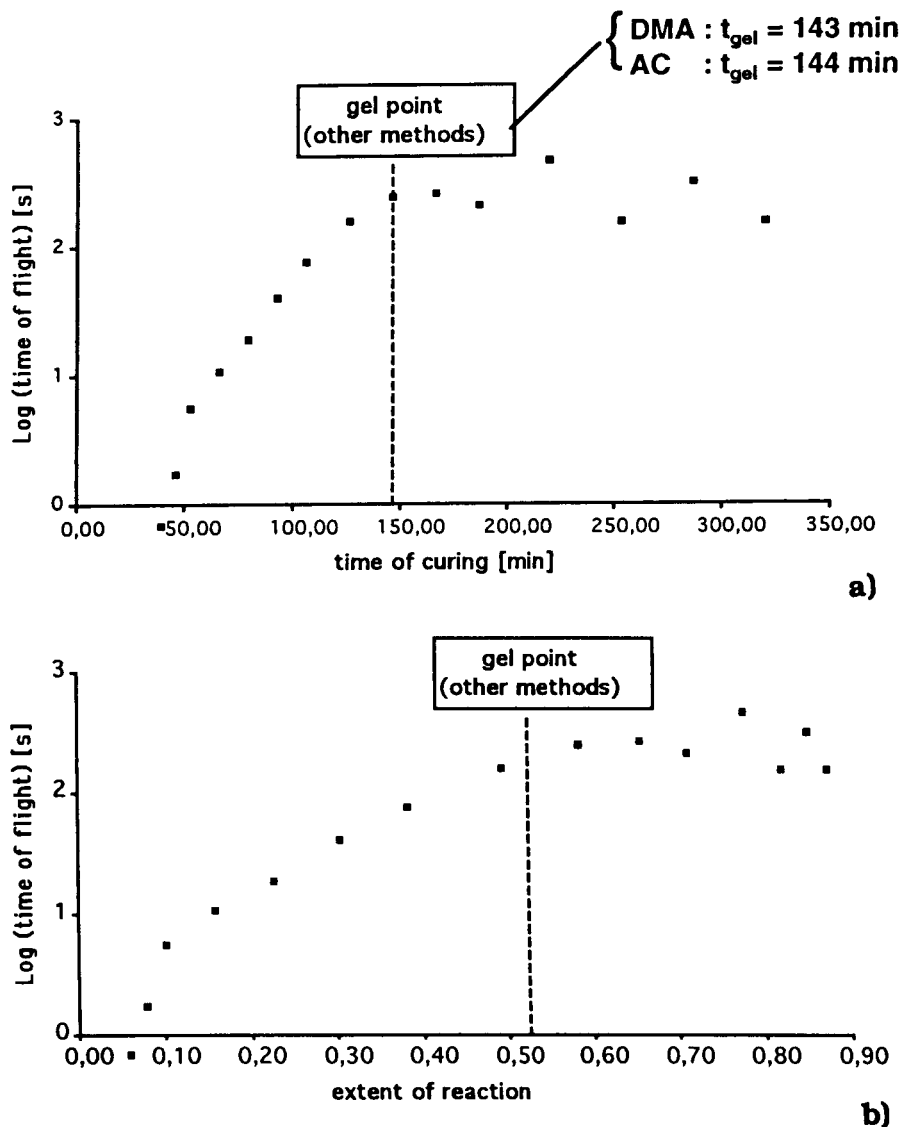


Figure 5 Plot of time of flight τ versus t or x for the epoxy system DGEBD-4D at 50°C.

where $\varepsilon_r - \varepsilon_u = \Delta\varepsilon$, (A , B) are constants depending on the electrode/polymer interface and taking into account the electrode polarizations' effects, n is a real number between 0 and 1, σ is the direct current (dc) conductivity, ε_o is the permittivity of free space (8.85×10^{-14} F/cm), ε_r is the relaxed dielectric permittivity, ε_u is the unrelaxed dielectric permittivity, τ is the relaxation time of the dipoles, and ω is the angular frequency.

When conduction effects predominate, then from eq. (1) $\varepsilon''\varepsilon_o\omega$ is independent of frequency. The reduction of conductivity during curing re-

ffects the increase of the resin viscosity. When the ionic conductivity is small, dipolar loss peaks can be observed.

In initially miscible epoxy systems blended with tougheners like elastomers³ or thermoplastics,^{10,20} a phase separation will occur under curing and yield biphasic materials. In these heterogeneous systems, the differences of conductivity and permittivity between two media produce an accumulation of charges' carriers at the interface and, as a result, the interfacial polarization. In the case of ellipsoids of conductivity σ_2 and permittivity ε_2 dispersed in a homogeneous matrix

(σ_1, ε_1), the dielectric properties are described by a MWS relaxation model.²⁸ The average relaxation time τ_{MWS} and the limiting permittivities ε_s and ε_o are a function of the dielectric properties of each phase, the volume fraction ν_2 of the dispersed phase, and a factor A_a that depends on the shape of the particles.

$$\tau_{\text{MWS}} = \left[\frac{\varepsilon_1 + A_a(1 - \nu_2)(\varepsilon_2 - \varepsilon_1)}{\sigma_1 + A_a(1 - \nu_2)(\sigma_2 - \sigma_1)} \right] \varepsilon_o$$

$$\varepsilon_s = \varepsilon_1 \frac{\sigma_1[A_a(1 - \nu_2) + \nu_2](\sigma_2 - \sigma_1)}{\sigma_1 + A_a(1 - \nu_2)(\sigma_2 - \sigma_1)}$$

$$+ \nu_2 \sigma_1 \frac{\sigma_1 + A_a(\sigma_2 - \sigma_1)(\varepsilon_2 - \varepsilon_1) - [\varepsilon_1 + A_a(\varepsilon_2 - \varepsilon_1)](\sigma_2 - \sigma_1)}{[\sigma_1 + A_a(1 - \nu_2)(\sigma_2 - \sigma_1)]^2}$$

$$\varepsilon_o = \varepsilon_1 \frac{\varepsilon_1 + [A_a(1 - \nu_2) + \nu_2](\varepsilon_2 - \varepsilon_1)}{\varepsilon_1 + A_a(1 - \nu_2)(\varepsilon_2 - \varepsilon_1)} \quad (2)$$

with spherical particles $A_a = \frac{1}{3}$.

In this work all the calculations are built on these equations. For many systems like epoxy-CTBN blends,^{7,21} simplifications are possible when the dispersed spherical particles are much more conductive than the matrix and when their volume fraction is small ($\sigma_1 \ll \sigma_2$ and $\nu_2 < 0.2$).

dc Measurements

The cure monitoring of thermoset matrix composites was performed using the new method of evaluation of ionic conductivity.²⁹ This consists of applying direct voltage to the sample instead of an alternate voltage.

Under the application of an alternative field, dielectric response includes ionic conductivity and dipolar motions, which was difficult to distinguish. The dc measurements allowed us to isolate the ionic contribution and study its evolution during the polymerization after the stabilization of dipolar currents.

An experimental device made of an electrometer with an incorporated voltage source (Keithley 617) and a ceramic single surface sensor was built to access the values of the current crossing the system. An IBM/PS2 computer was used to acquire, store, and process the experimental data.

To study the charging characteristics of a material, it is necessary to discharge the material prior to the beginning of the next charging process for at least 10 times longer than the maximum de-

sired time of the charge measurement.³⁰ That is the reason why after a charging time of 10 s the sample is short circuited during a discharging time of 100 s. That allows the removal of residual currents, the presence of which could arise from the accumulation of excess charges resulting from previous polarizations. This condition was satisfied for all the temperatures of the various studied cure cycles.

Time of Flight (TOF) Measurements

The ionic mobility can be evaluated from dc measurements on the cell with ion blocking electrodes.³¹ The dc voltage (U) is initially applied to the cell in one direction for a long time in order to accumulate all mobile ions in the vicinity of the electrodes. The polarity of the applied voltage is then reversed and the flowing current is recorded. When the ionic carriers reach the opposite electrode they will accumulate again near that electrode, leading to a decrease of the mobile ionic carrier's concentration and consequently to the decrease of the conduction current. If this decrease of current can be detected, it would allow the determination of an average TOF (τ) of ions over the sample thickness. Then, by taking into account the sample thickness (δ), it will be possible to calculate the ion mobility (μ) from eq. (3).

$$\mu = \frac{D^2}{\tau U} \quad (3)$$

The measuring circuit consisted of a Keithley 617 electrometer with incorporated voltage source, a PC computer for data acquisition, storage, and handling, and the thermoregulated measurement oven.

The sandwich-type configuration of the sample was chosen for these measurements; it had two parallel plate, round electrodes ($f = 16$ mm) with guard rings. These plates were distanced with polyethylene terephthalate (PET) films of different thicknesses (0.02–0.2 mm). The resin sample (which was a viscous liquid at the beginning) was placed between preheated plates and then put in the thermostatted oven. Various metals were used as the material of the electrodes: Cu, Ag, Al, Au.

Other Experiments

The kinetic analysis was performed by SEC and DSC. The rheological studies were performed on

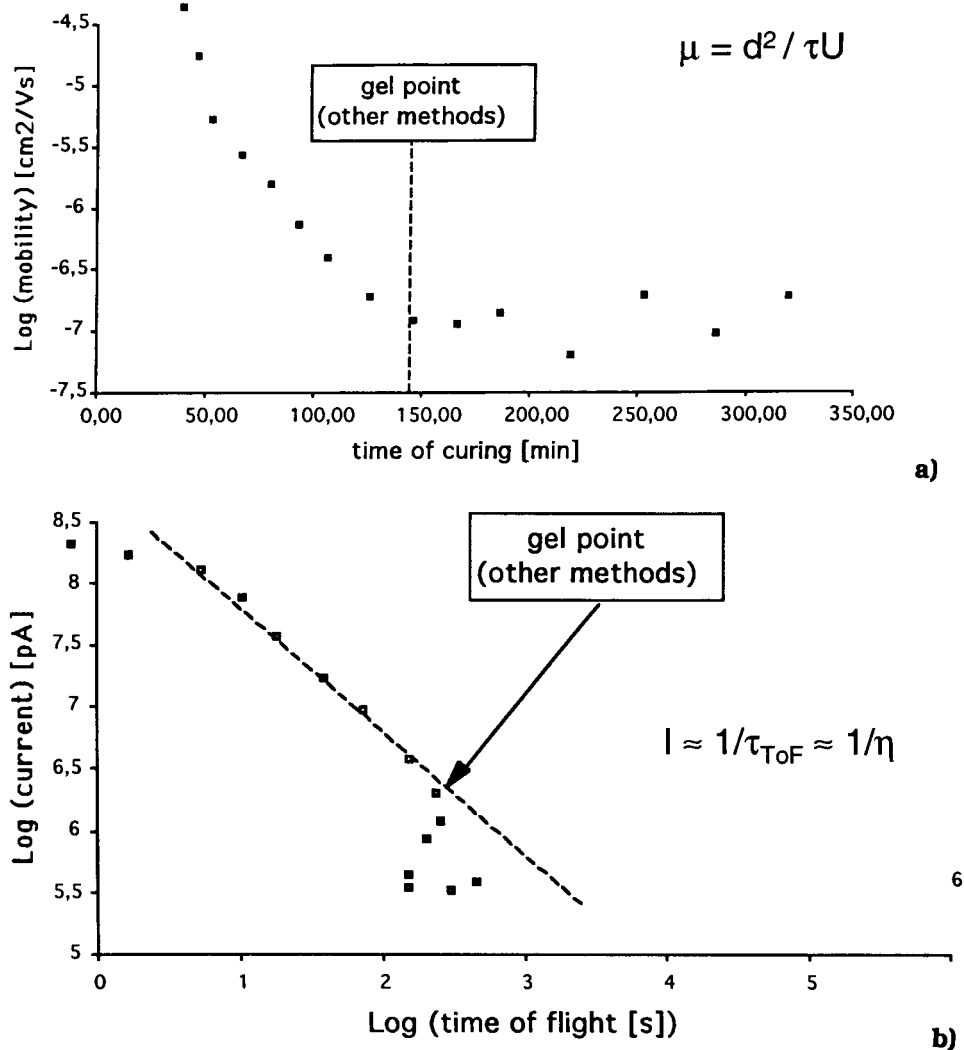


Figure 6 (a) Variation of log mobility versus time of cure and (b) log I versus log τ for the epoxy system DGEBD-4D at 50°C.

a Rheometrics RDA 2 and simultaneous experiments of the phase separation were made by the determination of the cloud point from light transmission experiments. The toughened samples were microtomed at room temperature and then the morphologies were identified by transmission electron microscopy (TEM) and phase contrast optical microscopy.

Materials

Epoxy Systems

The measurements' series were done for the following stoichiometric mixtures of the epoxy resin

systems isothermally cured at different temperatures:

- diglycidyl ether of 1,4-butanediol (DGEBD) with 4,9-dioxa-1,12-dodecane diamine (4D) for the gelation phenomenon only; and
- diglycidyl ether of bisphenol A (DGEBA) with diamino-4,4'-dimethyl-3,3'-dimethyl-dicyclohexylmethane (3DCM) for the gelation and vitrification phenomena.

Toughened Epoxies

The epoxy resin used was tetraglycidyl diamino diphenyl methane (TGDDM) from Ciba-Geigy

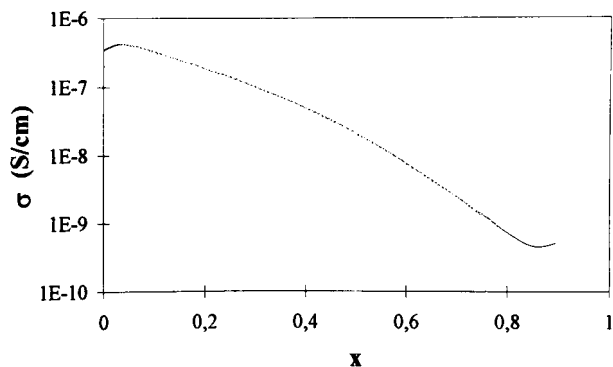


Figure 7 $\log \sigma$ versus conversion degree x for epoxy system DGEBD-4D at 50°C with IDEX sensor.

(MY721). The hardener was methylethyl aniline (MEA) from Lonza. The modifier was an amorphous nonreactive poly(etherimide) (PEI) produced by General Electrics Plastics (Ultem 1000) that had a glass transition temperature (T_g) at 214°C and number average molecular weights (M_n) of 50,000 and 26,000 g/mol. These values were measured elsewhere.³ A fine powder of PEI ($\theta < 160 \mu\text{m}$) was used for easy dissolving in this resin. The dielectric properties of PEI were measured at 160°C for a 125-mm thick film and were $\epsilon' = 4.5$ and $\sigma = 10^{-12}$ mho/m.

For the neat resin the epoxy resin and the hardener were mixed in a stoichiometric ratio at 90°C for 20 min until the mixture was clear and homogeneous.

A different procedure was used for the ternary blends. The PEI was dried for 4 h at 150°C and then dissolved in the epoxy resin at 140°C for 20 min. The blend was cooled to 100°C and then the hardener was added. Stirring for 20 min at 90°C was necessary to homogenize the blend. The reaction during this stage was negligible. This process is interesting because it does not need the use of a solvent. The experiments were carried out on blends of various compositions (from 0 to 20.9 wt % PEI) at 160°C.

Polyamides

Two polyamides, A and B (Rhône Poulenc), were used. The B-type polyamide contained a nucleating agent.

RESULTS AND DISCUSSION

Epoxies

The alternating current (ac), dc, and TOF measurements were performed on the DGEBA-3DCM

system. The ac measurements were done on the DGEBA-MDEA system as well. The variation of $\log(\sigma)$ versus time of curing or versus conversion (i.e., the degree of the polycondensation calculated by the relation of Runge–Kutta using the parameter of the kinetics³²) was plotted in Figure 1(a,b). On these ac spectra one can see a decrease of the conductivity during cure down to a 10^{-10} level. It was possible to measure with the IDEX sensor, although we had problems with the limit of sensitivity of the sensor on the insulating cured system.

The superposition of the curves at the beginning of cure for different frequencies indicated that the ionic process of conduction was dominant. With proceeding of the reaction the viscosity increased and the mobility of the ionic species decreased. These curves showed additional peaks according to the rule that the higher the frequency is, the earlier the peaks appear. This effect is the result of the dipolar relaxation related to the vitrification of the chain segments.^{3,16,33}

In previous work^{6,34} we showed that for the model DGEBA-3DCM system it was possible to detect an inflexion point on the $\log(I)$ curves plotted versus time near the gelation [Fig. 1(a)]. It was found later³⁵ that there are other types of systems where this inflexion point appears before gelation and that this indicator in the pregel region can be useful in the industrial process. The debate on interpretation of this particular point is ongoing.^{36,37}

In this aspect, it is interesting, knowing the kinetic of the system under cure, to plot the conductivity versus the degree of conversion. As shown in Figure 1(b), one cannot see any inflexion point on such a representation.

The CHIP sensor increased the sensitivity of the technique and our measurements, especially at high conversion level; its presentation on the curve represents the same variations after extraction of the dipolar effect (Fig. 2).

A better insight into the appearance of the inflexion point on the curve versus time was observed [Fig. 2(a)] and we cannot relate this to the limitation of the conductivity. This inflexion point disappeared in the representation versus degree of conversion [Fig. 2(b)].

The other dc measurement experiments were performed with a patented method from our laboratory.²⁹ The example results for the model DGEBA-3DCM system cured at different temper-

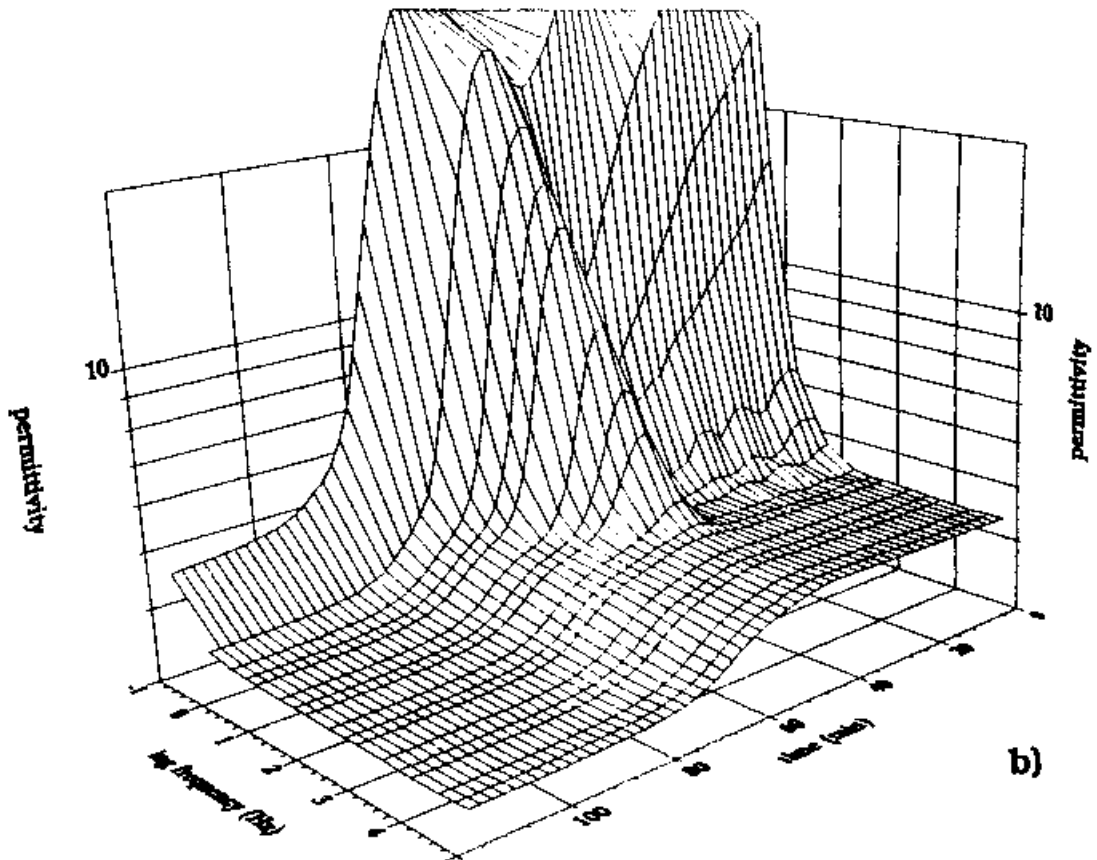
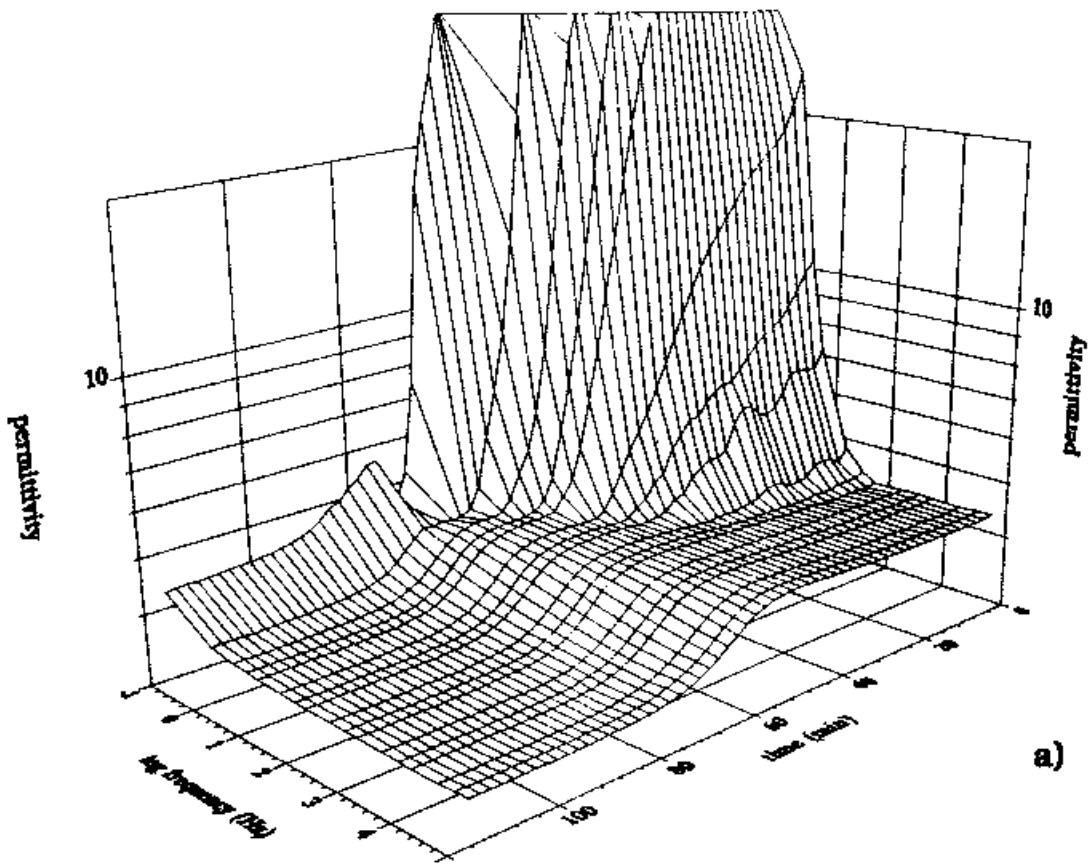


Figure 8 Plots of permittivity versus time for different blends of TGDDM-MEA at different contents of PEI.

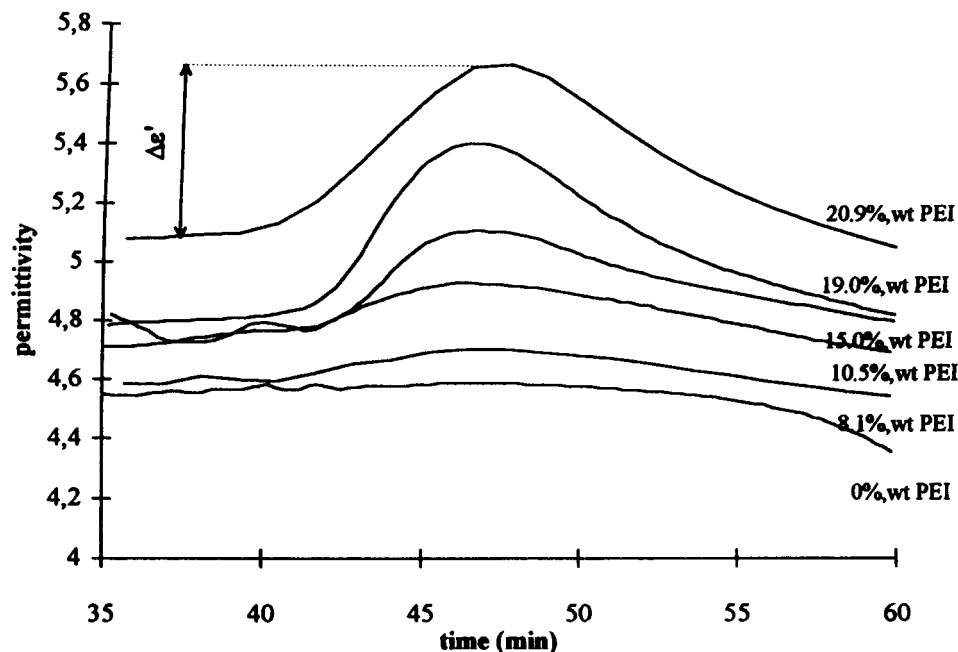


Figure 9 (a) 3-D spectra of neat TGDDM-MDEA and (b) toughened epoxy TGDDM-MEA-PEI.

atures are plotted versus time in Figure 3(a) and versus degree of conversion in Figure 3(b).

This method gives very sensitive results over 70 degrees of magnitude of the static currents. The inflexion point is well detected for the temperature range of 80–100°C and for the isothermal conditions when the gelation is a phenomenon that appears far from the vitrification time. It is not true for the temperature range of 60–70°C because of the vitrification phenomenon that is close to gelification. Similar conclusions can be drawn as previously for the curves plotted as the function of degree of conversion.

Finally, the DGEBA-3DCM system was examined with the TOF technique.³¹

The current signals obtained in the TOF experiments correlate strongly with the material of the electrodes. They must be ion blocking electrodes for the mobile ionic species present in the medium. It is possible to find experimental conditions (nature of the electrode, field strength, sample thickness, temperature) in which a distinct kink in the $I(t)$ curve and some times a maximum is observed. This moment can be regarded as the time when ionic carriers, checked in the medium, have reached the opposite electrode. This causes a decrease in the number of mobile ions in the bulk (clean-up effect) and a decrease of the inter-

nal electric field (space charge effect). Thus, the number of mobile ions in the bulk reaches maximum at some time (τ); therefore, the time dependence of the monitored current also shows a peak.¹²

According to the concept of TOF, the time τ should increase with an increase of the sample thickness (for the same voltage) and the TOF of the ionic carriers should decrease with an increase of the electric field (for the constant distance layer). These effects are presented in the literature³¹ and confirm our interpretation of the TOF experiment results.

In the investigated DGEBA-3DCM resin system it was found, as expected, that the ionic conductivity decreased with an advancement of the reaction. According to our predictions, the TOF of ionic carriers should increase with the advancement of the reaction as a result of an increase of the medium viscosity in the course of curing. The higher the viscosity is, the lower the mobility of the ionic carriers is and a longer time is needed by them to reach the opposite electrode. The plot of $\log(I)$ versus $\log(\tau)$ gives an approximate straight line with a slope of -1 (Fig. 4), indicating linear relations between the ionic conductivity and mobility in this range of advancement of the reaction, that is, before reaching the gelation point.

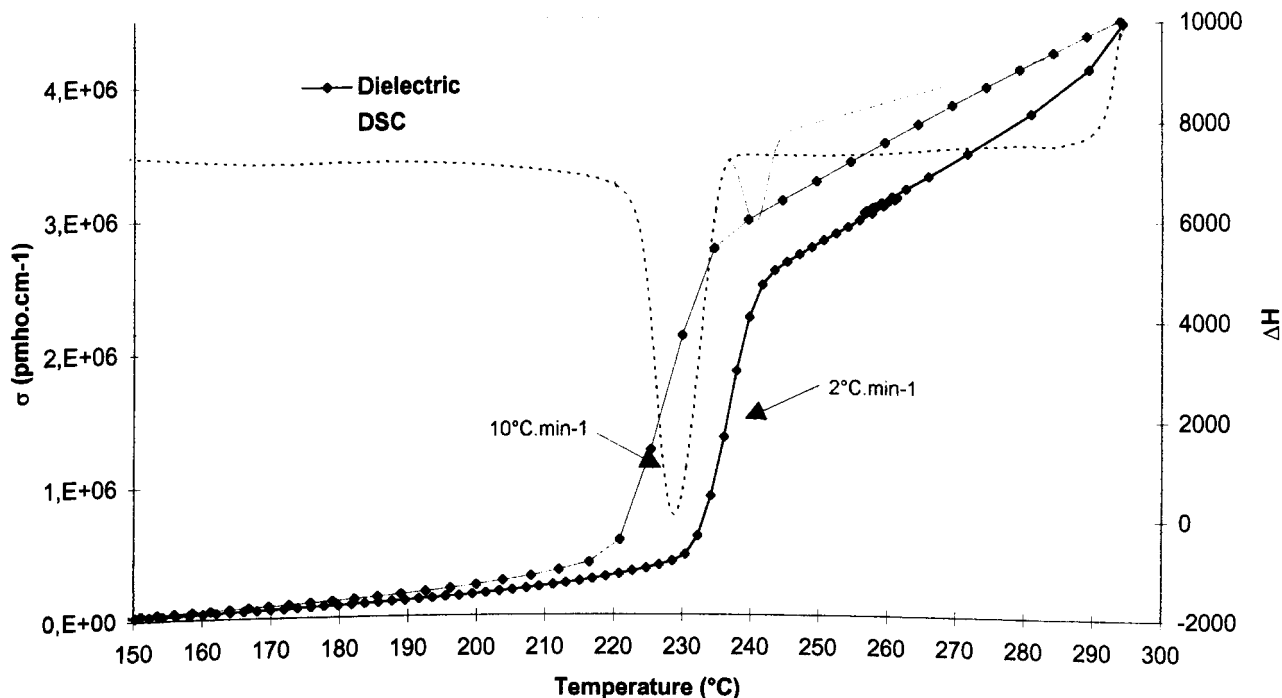


Figure 10 Conductivity and DSC spectra during the crystallization of a polyamide at two different rates of cooling.

The evolution of the ionic carriers' mobility versus time of curing, calculated according to eq. (3), did not show changes as the resin was approaching gelation. The ion carriers' mobility decreased so strongly (i.e., the TOF became very long and exceeded the time of polarization), that it was not possible to follow the changes in the ion mobility through and above the gelation phenomena, even when changing the experimental conditions.

The experiments carried out on the DGEBD-4D systems were encouraging because the level of the conductivity was sufficiently high (less viscous, low T_g epoxy-amine system, above room temperature only gelation occurs). The TOF conditions of the measurement were able to follow the curing of this system (Fig. 5). It is clear that whatever the values plotted on the abscissa axis, time [Fig. 5(a)] or degree of conversion [Fig. 5(b)], the gelation influenced the TOF of the ions crossing the medium.

Figure 6(a) plots the real values of the ions' mobility versus time of curing. The results show that the linear relation between the $\log(\text{current})$ and the $\log(\text{TOF})$ is no more respected above gelation [Fig. 6(b)]. The mobility seems to stay constant after gelation. Therefore, the observed de-

crease of the conductivity suggests some decrease of the number of mobile ions (Fig. 5).

Comparing this hypothesis with the evolution of the conductivity in the conversion in Figure 7, it can explain the amplification of the decrease of the conductivity in the gelation area.

Toughened Epoxies

Figure 8(a) presents 3-D plots of the permittivity of the neat resin-hardener mixture during cure at 160°C. At the beginning of the reaction, the permittivity exhibits very high values at low frequencies, reflecting an electrode polarization. This phenomenon is the result of the high conductivity of the resin due to its low viscosity and the presence of ionic species. As the viscosity of the resin increases, the electrode polarization lessens and allows the dipolar contribution on permittivity to appear. As the resin changes from the gel to the glassy state, the permittivity decreases with a step (and the loss factor curves present at the same time a peak depending on the frequency). This dipolar relaxation is generally attributed to the buildup of the α relaxation of the epoxy network.^{3,16}

The modified resin TGDDM-MDEA blend con-

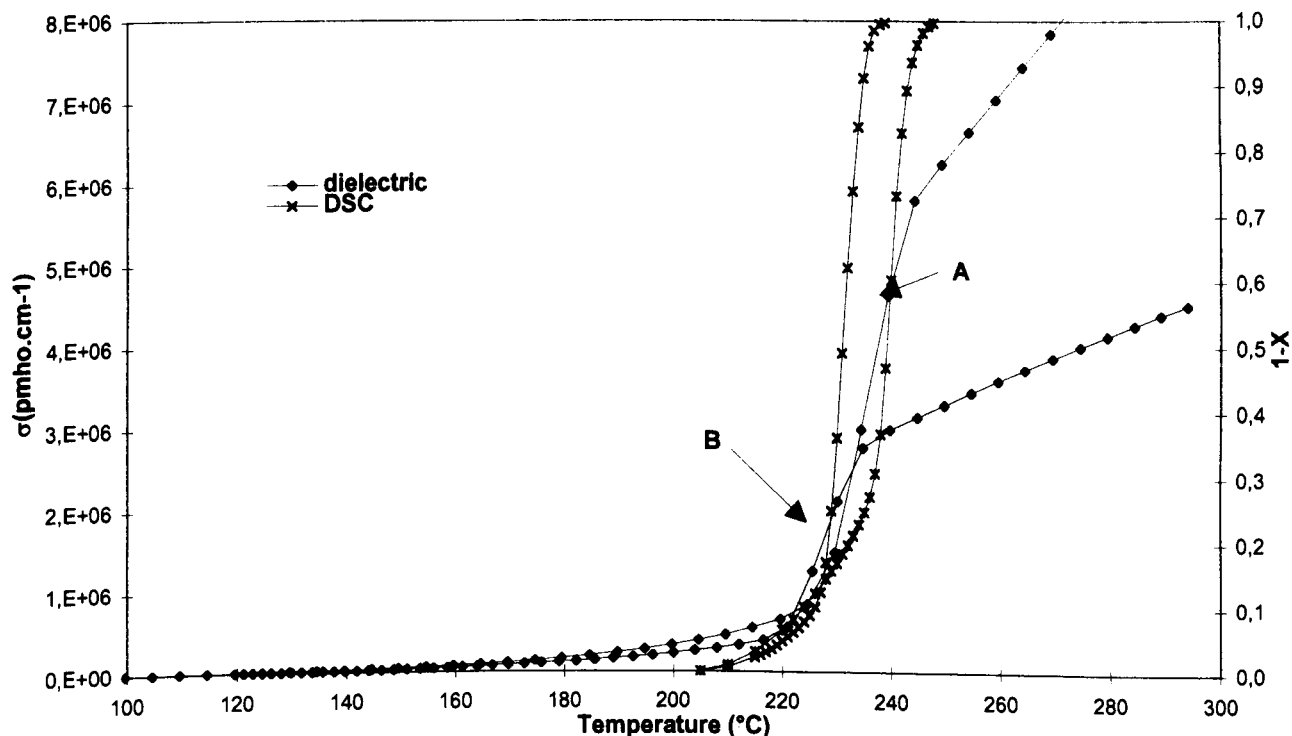


Figure 11 Conductivity and DSC spectra during the crystallization of polyamide A and polyamide B (A with nucleating agent).

taining 20.9% PEI in Figure 8(b) shows that the initial values of permittivity at high frequencies are not modified by the presence of PEI in the epoxy but are from the initial conductivity of the blend being lowered with the PEI. (The higher viscosity of the blend is certainly the main cause for this; the electrode polarization effect is slightly reduced at low frequency measurements.)

When the phase separation begins, the permittivity at low frequencies increases sharply, resulting from the interfacial polarization observed with several epoxy blends that exhibit a phase separation.^{4,7,38}

When the phase separation takes place in the mixtures with PEI, the interfacial polarization does not remain constant with curing time because of the variations of the following factors: permittivities and conductivities of each phase, volume fraction, and shape and size of the dispersed phase. Therefore, it is difficult to quantify the evolution of the interfacial polarization.

Phase separation takes place creating two phases: the epoxy-amine rich phase that will be called the α phase and the PEI rich phase labeled the β phase. During the phase separation, the composition of each phase changes because of

thermodynamics; consequently, their viscosities and conductivities evolve. The α phase becomes poorer and the β phase becomes richer in PEI.

Because the molar mass of the resin is still much smaller than that of the PEI, the viscosity of the α phase automatically decreases and the β phase one increases. (That is the main difference from epoxy-elastomer blends where the contrary occurs.) In terms of dielectrometry, the conductivity of the pure PEI is much lower than the one of the neat resin at this extent of reaction. One can conclude that the variation of composition in each phase causes an increase of the conductivity of the α phase and a decrease of β phase one. This effect theoretically results in an emphasis of the interfacial polarization, because the difference between the conductivities of the phases increases.

The second effect affecting the conductivities of the phases is the polymerization of the resin. In the cure of the neat resin, the conductivity decreases as the polymerization proceeds. Therefore, both conductivities of the two phases follow this evolution; but the α phase, which is richer in epoxy-amine, is much more affected by this contribution.

The variations of composition in the phases and

the polymerization of the resin have two opposite effects that compete to govern the interfacial polarization.

The influence of the volume fraction of PEI in the epoxy matrix on the interfacial polarization depends on the geometry of the system²⁸ and the shape of the interface that determines its faculty to trap some charge carriers.

We expect to have different dielectric responses during the formation of different morphologies. Moreover, the evolution of the volume fraction during the phase separation depends on the initial concentration of PEI and on the phase diagram.^{33,38,39}

Figure 9 presents the evolution of the permittivity at 100 Hz for several blends. The permittivity peak grows if the quantity of PEI is increased. We call $\Delta\epsilon'$ the permittivity jump occurring during the phase separation at a given frequency. This is considered as a parameter representative of the intensity of the interfacial polarization. On the basis of observation of Maistros et al.,⁷ we normalized $\Delta\epsilon'$ with σ_{cp} , corresponding to the conductivity at the cloud point.²² Thus, it is possible to identify radical changes of morphology like the phase inversion.

Polyamides

A dielectric study of the crystallization of polyamide 6-6 was conducted. The real time evolution of conductivity extracted from the loss factor from 300 to 150°C at different cooling rates are reported in Figure 10 for sample A. We can note the good agreement of this evolution with the exothermic peak of crystallization for the two cooling rates used. Another analysis was carried out on the same polyamide with and without nucleating agent.

Figure 11 shows the electrical response and the transformation ratio obtained by DSC analysis at the same cooling rate. It confirms that the crystallization starts at the same temperature and that the dielectric study is more sensitive to the secondary crystallization than DSC analysis. Actually these first experiments were carried out on the analysis of dielectric strength during the crystallization. At the same time, we developed an instrumented mold to examine the possibility of using an electric sensor in injection processing of thermoplastics.

CONCLUSION

To study the buildup of polymer networks and crystallization of thermoplastics, we performed different electrical studies on models and more complex reactive systems.

The evolution of different electrical parameters was checked as being representative of chemical or physical events.

Our goal was to understand the modification of ionic and molecular mobility during such events. The gelation and the vitrification phenomena were approached through polymerization of epoxy.

The concept of TOF was applied for determination of ion mobility in a reactive polymer medium and gave some insights into the mechanism of ionic conductivity evolution in the course of curing.

Dielectric measurements detected the phase separation, which was induced by the polymerization of a thermoplastic-modified epoxy, and appeared to be more sensitive than the classical cloud point experiments.

Finally, the physical transition characteristic like crystallization of a thermoplastic material is a suitable phenomenon to be followed by the *in situ* techniques. This opens new perspectives in the control of the process of such materials.

The authors thank the MRES, the Polish State Committee for Scientific Research (Grant 607/T08/96/10), and the DRET (September 1991–February 1993), DGA, for the financial support of Krzysztof Friedrich and the Society Brochier for the financial support of Cyril Vinh–Tung.

REFERENCES

1. S. D. Senturia and N. F. Sheppard, Jr., *Adv. Polym. Sci.*, **80**, 1 (1986).
2. T. Koike, *J. Appl. Polym. Sci.*, **50**, 1943 (1993).
3. M. B. M. Mangion and G. P. Johari, *J. Polym. Sci., Polym. Phys.*, **29**, 1117 (1991).
4. C. G. Delides, D. Hayward, R. A. Pethrick, and A. S. Vatalis, *Eur. Polym. J.*, **28**, 505 (1992).
5. D. Kranbuehl, S. Delos, M. Hoff, and P. Haverty, *Polym. Eng. Sci.*, **29**, 285 (1989).
6. G. Boiteux, P. Dublineau, M. Fève, C. Mathieu, G. Seytre, and J. Ulanski, *Polym. Bull.*, **30**, 441 (1993).
7. G. Maistros, H. Block, C. Bucknall, and I. Partridge, *Polymer*, **33**, 4470 (1992).

8. J. Simpson and S. A. Bidstrup, *J. Polym. Sci., Polym. Phys.*, **33**, 55 (1995).
9. J. Simpson and S. A. Bidstrup, *J. Polym. Sci., Polym. Phys.*, **31**, 609 (1993).
10. A. MacKinnon, S. Jenkins, P. McGrail, and R. Pethrick, *Polymer*, **34**, 3252 (1993).
11. I. Alig and G. P. Johari, *J. Polym. Sci., Polym. Phys.*, **31**, 299 (1993).
12. M. Watanabe, K. Sanui, N. Ogata, F. Inoue, T. Kobayashi, and Z. Ohtaki, *Polym. J.*, **17**, 549 (1985).
13. M. Watanabe, M. Rikukawa, K. Sanui, and N. Ogata, *J. Appl. Phys.*, **58**, 736 (1985).
14. H. W. Starkweather, Jr. and P. Avakian, *Macromolecules*, **26**, 6217 (1993).
15. Y. Zheng and G. Wan, *J. Appl. Polym. Sci.*, **57**, 623 (1995).
16. Y. Deng and G. Martin, *Macromolecules*, **27**, 5141 (1994), **27**, 5147 (1994).
17. J. Mijovic, *Polym. Mater. Sci. Eng.*, **72**, 54 (1995).
18. F. Stephan, G. Boiteux, and G. Seytre, *Mater. Tech.*, **Novembre-Décembre** (1994).
19. G. Korkakas, C. M. Gomez, and C. B. Bucknall, *Plast. Rubber Comp. Process. Appl.*, **19**, 285 (1993).
20. A. J. MacKinnon, S. D. Jenkins, P. T. McGrail, and R. A. Pethrick, *Macromolecules*, **25**, 3492 (1992).
21. E. Girard-Reydet, C. C. Riccardi, H. Sautereau, and J. P. Pascault, *Macromolecules*, **28**, 7608 (1995).
22. C. Vinh-Tung, G. Boiteux, G. Seytre, G. Lachenal, and B. Chabert, *Polym. Compos.*, **17**, 761 (1996).
23. D. E. Kranbuehl, S. E. Delos, M. S. Hoff, L. W. Weller, P. D. Haverty, J. A. Seeley, and B. A. Whitham, article presented at the 32nd International SAMPE, April 6-9, 1987.
24. T. A. Ezquerra, F. J. Balta-Calleja, and H. G. Zachmann, *Polymer*, **35**, 2600 (1994).
25. T. A. Ezquerra, Z. Roslaniec, E. Lopez-Cabarcos, and F. J. Balta Calleja, *Macromolecules*, **28**, 4516 (1995).
26. J. C. Coburn and R. H. Boyd, *Macromolecules*, **19**, 2238 (1986).
27. D. A. Seanor, *Electrical Properties of Polymers*, Academic Press, New York, 1982.
28. L. K. H. Van Beck, *Prog. Dielectr.*, **7**, 69 (1967).
29. F. Stephan, G. Seytre, G. Boiteux, J. Ulanski, and J. Y. Chatelier, Fr. Pat. 9,503,399 (1995).
30. A. K. Jonscher, *Dielectric Relaxation in Solids*, Chelsea Dielectrics Press, London, 1983.
31. J. Ulanski, K. Friedrich, G. Boiteux, and G. Seytre, *J. Appl. Polym. Sci.*, to appear.
32. D. Verchère, H. Sautereau, J. P. Pascault, S. M. Moschiar, C. C. Riccardi, and R. J. J. Williams, *Polymer*, **30**, 107 (1989).
33. G. Williams, C. Duch, J. Fournier, and J. R. Hayden, *Polymer Spectroscopy*, A. H. Fawcett, Ed., Wiley, Chichester, England, 1996, p. 275.
34. G. Boiteux, G. Seytre, C. Mathieu, R. Villain, and P. Dublineau, *J. Non-Cryst. Solids*, **172-174**, 1012 (1994).
35. D. Kranbuehl, D. Hood, Y. Wang, G. Boiteux, F. Stephan, C. Mathieu, G. Seytre, A. Loos, and D. Mc Rae, *Polym. Adv. Technol.*, to appear.
36. J. Mijovic, S. Andjelic, B. Fitz, W. Zurawsky, I. Mondragon, F. Bellucci, and L. Nicolais, *J. Polym. Sci.: Part B*, **34**, 379 (1996).
37. J. Mijovic and F. Bellucci, *TRIP*, **4** (1996).
38. M. L. Wang, G. P. Johari, and J. P. Szabo, *Polymer*, **33**, 4747 (1992).
39. R. A. Ruseckaite and R. J. J. Williams, *Polym. Int.*, **30**, 11 (1993).